Charge dynamics in the 2D/3D semiconductor heterostructure WSe_2/GaAs

Rojas-Lopez, Rafael R.; Hendriks, Freddie; van der Wal, Caspar H.; Guimarães, Paulo S.S.; Guimarães, Marcos H.D.

Published in:
Applied Physics Letters

DOI:
10.1063/5.0214767

Publication date:
2024

RESEARCH ARTICLE | SEPTEMBER 23 2024

Charge dynamics in the 2D/3D semiconductor heterostructure WSe_2/GaAs

Rafael R. Rojas-Lopez ; Freddie Hendriks ; Caspar H. van der Wal ; Paulo S. S. Guimarães ; Marcos H. D. Guimarães

Appl. Phys. Lett. 125, 132104 (2024)
https://doi.org/10.1063/5.0214767

Applied Physics Letters ARTICLE pubs.aip.org/aip/apl

Charge dynamics in the 2D/3D semiconductor heterostructure WSe_2/GaAs

Cite as: Appl. Phys. Lett. **125**, 132104 (2024); doi: 10.1063/5.0214767
Submitted: 19 April 2024 · Accepted: 12 September 2024 ·
Published Online: 23 September 2024

View Online Export Citation CrossMark

Rafael R. Rojas-Lopez,[1,2,a)] Freddie Hendriks,[1] Caspar H. van der Wal,[1] Paulo S. S. Guimarães,[2] and Marcos H. D. Guimarães[1,a)]

AFFILIATIONS

[1]Zernike Institute for Advanced Materials, University of Groningen, 9747 AG Groningen, The Netherlands
[2]Departamento de Física, Universidade Federal de Minas Gerais, 31270-901 Belo Horizonte, Brazil

[a)]**Authors to whom correspondence should be addressed:** rrlopez@fisica.ufmg.br and m.h.guimaraes@rug.nl

ABSTRACT

Understanding the relaxation and recombination processes of excited states in two-dimensional (2D)/three-dimensional (3D) semiconductor heterojunctions is essential for developing efficient optical and (opto)electronic devices, which integrate van der Waals 2D materials with more conventional 3D ones. In this work, we unveil the carrier dynamics and charge transfer in a monolayer of WSe_2 on a GaAs substrate. We use time-resolved differential reflectivity to study the charge relaxation processes involved in the junction and how they change when compared to an electrically decoupled heterostructure, WSe_2/hBN/GaAs. We observe that the monolayer in direct contact with the GaAs substrate presents longer optically excited carrier lifetimes (3.5 ns) when compared with the hBN-isolated region (1 ns), consistent with a strong reduction of radiative decay and a fast charge transfer of a single polarity. Through low-temperature measurements, we find evidence of a type-II band alignment for this heterostructure with an exciton dissociation that accumulates electrons in GaAs and holes in WSe_2. The type-II band alignment and fast photoexcited carrier dissociation shown here indicate that WSe_2/GaAs is a promising junction for advanced photovoltaic and other optoelectronic devices, making use of the best properties of van der Waals (2D) and conventional (3D) semiconductors.

Monolayer transition metal dichalcogenides (TMDs) have received a lot of attention because of their atomically thin thickness and interesting optical and electronic properties.[1–3] Their thickness confines the charges in the plane of the monolayer, resulting in strikingly different properties from their bulk counterpart.[3–5] Additionally, the stacking and/or twisting of consecutive monolayers into heterostructures has been shown to give rise to unique physical phenomena and makes them strong candidates for the next generation of nanodevices.[6,7] Their low dimensionality also makes them very sensitive to local changes, such as defects in the crystal lattice, strain, or impurities.[8–10] The interaction with the environment can also modify the properties of the two-dimensional (2D) semiconductor through, for instance, the interaction with gases or substrates with different electronic properties.[11,12] The dielectric environment for the Coulomb interaction that gives place to excitonic phenomena in TMDs is particularly important and has been shown to be able to modulate its optical properties.[13] Therefore, we can use this as an advantage for developing nanodevices such as gas sensors, photodetectors, and solar cells.[14–16]

Gallium arsenide (GaAs) is one of the most studied semiconductors because of its applications in electronics as well as its very high electronic mobility, which allows for efficient gate-induced quantum confinement to one or two dimensions.[17] In particular, previous studies have demonstrated that the junction of this three-dimensional (3D) semiconductor with TMDs (i.e., 2D semiconductors) is a promising junction for optoelectronic devices.[15,16,18–20] In order to optimize and manipulate such systems for improving the design of the next generation of (opto)electronic devices, we need to obtain a high level of understanding of the electronic properties and time evolution of their excited states. Nonetheless, the charge dynamics and band alignment between these materials are still largely unexplored.[21]

In this work, we study the carrier dynamics of the 2D/3D semiconductor heterojunction WSe_2/GaAs. We use an optical pump–probe approach, by measuring the time-resolved differential reflectivity (TRDR) of the junction and compare it with an electrically isolated WSe_2, by adding a hexagonal boron nitride (hBN) layer [Fig. 1(a)]. The WSe_2 monolayer in direct contact with GaAs shows carriers that decay much slower with respect to the isolated WSe_2 at low temperatures. This can be understood through a type-II band alignment that dissociates the optically excited excitons and creates an excess of electrons in the GaAs substrate and an excess of holes in the WSe_2 layer.

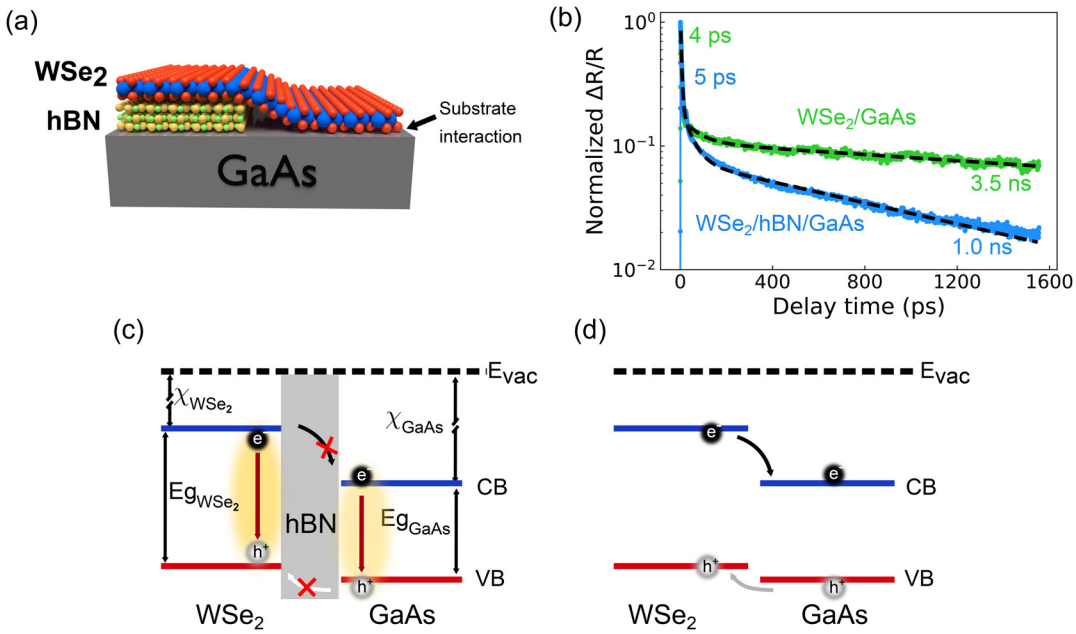

FIG. 1. (a) Schematics of our sample indicating the two regions of interest WSe_2/hBN/GaAs and WSe_2/GaAs. (b) Normalized differential reflectivity of the two regions using a laser wavelength in resonance with the WSe_2 exciton energy at each region: 705 nm for WSe_2/GaAs and 708 nm for WSe_2/hBN/GaAs. (c) Estimated band alignment of the 2D/3D semiconductor heterojunction with and (d) without considering the hBN electrostatic barrier. Here, E_{vac} represents the vacuum energy, CB the energy of the bottom of the conduction band, VB the top of the valence band, Eg the bandgap, and χ the electron affinity of the material. With a bandgap $Eg_{hBN} = 5.25$ eV and an electron affinity of $\chi_{hBN} = 2$ eV,[22] the hBN conduction and valence bands are out of the diagram scale and create a barrier that prevents the electron and hole carrier transfer between the materials, resulting in a dynamic dominated by the direct recombination of excitons. In (d), the absence of the hBN allows the exciton dissociation and carrier transfer in the heterojunction.

Nonetheless, at room temperature, we did not observe any important differences in the dynamics between the two regions, indicating a strong role of thermal effects on the relaxation process of photoexcited carriers.

Our samples were fabricated by mechanical exfoliation of WSe_2 and hBN from their bulk crystals (supplied by HQ Graphene). The hBN flakes were exfoliated with Nitto tape directly onto a commercial undoped (100) GaAs substrate (supplied by Wafer Technology) previously cleaned with argon plasma for 15 min, at a 0.1 mbar pressure, 250 W ICP (inductively coupled plasma) power and 5 W RF (radio frequency) power. The WSe_2 monolayers were exfoliated on a viscoelastic gel (Gel Pack) and then transferred on top of the hBN flake in the GaAs substrate with a van der Waals assembly setup (HQ Graphene).[23] We identified WSe_2 monolayers by optical contrast and photoluminescence in an optical microscope. The hBN thickness for the sample for which the results are shown here was (20 ± 2) nm, determined by atomic force microscopy. See the supplementary material for further characterization details. Time-resolved measurements were performed with a tunable Ti:sapphire pulsed laser with a pulse width <300 fs. We used a single-color (degenerate) pump–probe technique in a double modulation configuration as described in detail in our previous works.[24,25] We set the pump and probe beams to a 4:1 fluence ratio with a probe fluence of $6\,\mu J\,cm^{-2}$ in a $\sim 3\,\mu m^2$ active area. All measurements were carried out at a temperature of 70 K unless otherwise indicated.

Figure 1(b) shows the normalized TRDR of the two regions of the sample: the direct contact (WSe_2/GaAs—green) and the isolated (WSe_2/hBN/GaAs—blue) heterostructures when excited in resonance with the exciton transition of the WSe_2 layer as identified by TRDR spectroscopy (see below). Our results are well described by a three-processes exponential decay fit, $\Delta R/R = \sum R_{0i} e^{-t/\tau_i}$, with i from 1 to 3. Such multi-exponential decays have been reported by several works in the literature, but the origin of the different decay processes has been attributed to various sources, depending on the specifics of the system. Overall, it has been observed that radiative processes occur in no longer than a few hundred picoseconds, while non-radiative phenomena may last longer.[26–30] Here, we would like to highlight that TRDR, in contrast to time-resolved photoluminescence measurements, allows us to measure excited states of the system beyond the radiative phenomena. This direct relation with the absorption processes of the sample enables us to study the relaxation of both bound and not-bound excited states.

From our results, we observe a longer-lived component determined to be (3.50 ± 0.04) ns in the region of direct contact compared with (1.00 ± 0.01) ns for the isolated one. To understand the origin of this difference, it is necessary to look into the bandgap alignment between the materials as it provides a picture of the possible charge dynamics in a junction. For instance, previous reports observed that a junction of semiconductors with a type-I band alignment can result in a reduction of the lifetime of the material with the larger bandgap when placed in such a junction.[31,32] This phenomenon can be associated with an energy transfer process where, for instance, the optically generated exciton in one material transfers energy generating an exciton in the other material.[33] On the other hand, a type-II band offset

has been observed to increase the lifetime of the studied process,[30,34] including a report of carrier dynamics on the WS_2/GaAs heterojunction.[21] In those cases, the photo-generated excitons dissociate, resulting in a charge transfer, with electrons lying in one material and holes in the other. In light of this, we propose that our measurements point toward the existence of a type-II band offset in the WSe_2/GaAs heterojunction.

Simple band alignment estimations, as shown in Figs. 1(c) and 1(d), further corroborate the proposed type-II band offset between monolayer WSe_2 and GaAs. Here, we consider an electron affinity of 3.3 eV and an electronic bandgap of 2.08 eV for WSe_2 at room temperature, and $\chi_{WSe_2} = 3.26$ eV and $Eg_{WSe_2} = 2.16$ eV at 70 K based on previous reports (see supplementary material Note 3 for details).[35,36] While the bandgap E_g and electronic affinity χ of GaAs are well established in the literature, for WSe_2 these values can change from one reference to another. The sensitivity of monolayer TMDs with the electric environment and other experimental and theoretical details can lead to variation in these values, making it challenging for an accurate determination of these properties in a generic fashion. Nevertheless, even if differences in the exact values may arise, we can set an upper boundary for a type-II band offset. For this condition, the valence band maximum of WSe_2 has to be higher than the valence band of GaAs: $\chi_{WSe_2} + E_{g(WSe_2)} < 5.49$ eV at room temperature, or in general $\chi_{WSe_2}(T) + E_{g(WSe_2)}(T) < \chi_{GaAs}(T) + E_{g(GaAs)}(T)$. For simplicity, here we do not take into account band bending effects due to surface states or static charge transfer, which should be considered for a more accurate model.

This type-II band alignment implies a dissociation of photoexcited carriers with a charge transfer between the two materials. When the junction—monolayer and substrate—is excited, electrons at the conduction band will accumulate in the GaAs substrate, while the holes in the valence band will concentrate in the WSe_2 monolayer [Fig. 1(d)]. As a result, longer lifetimes of the excited states can be linked to a larger role of non-radiative scattering processes and a lack of available states in the valence (conduction) band for electrons (holes) to relax radiatively. The free carriers become then more prone to, for instance, a phonon- or defect-assisted recombination process where electrons return to the monolayer to recombine with the holes in the valence band.

In contrast, when considering the case of a WSe_2 isolated by hBN, charge transfer is restrained, and as a result, radiative exciton recombination is again the faster pathway for the relaxation of carriers [see Fig. 1(c)]. Therefore, our results point toward a photoexcited carrier transfer between GaAs and WSe_2. We expect this process to take place at the Γ point in the valence band, and the Λ point in the conduction band of WSe_2, via a phonon-assisted mechanism.[37]

In Fig. 1(b), we also observe a fast decay time (τ_1) of 4 ps for WSe_2 in direct contact with GaAs and 5 ps for the isolated region. We attribute this fast process in part to a stimulated emission, related to our single-color pump–probe excitation, as well as to exciton recombination out of thermal equilibrium.[26–28,38] Despite the resolution of our measurements, we cannot associate the small difference in the τ_1 relaxation times as arising exclusively from the interaction with the substrate, as stress or defects in the monolayer can modify the charge dynamics within the observed difference. Finally, we observed an intermediate decay time (τ_2) of 90 ps for the monolayer in direct contact and 50 ps in the isolated region, consistent with previous measurements of trion recombination lifetime.[27,29] We associate the difference in the relaxation times τ_2 with an increase in the density of one type of charge carrier in WSe_2 that protects the trion from fast recombination. In particular, in our sample, two phenomena can give origin to this imbalance of carriers: the reduction in the Fermi level of WSe_2 due to the formation of the joint-Fermi level of the heterojunction with GaAs, and the dissociation and charge transfer from the photoexcited carriers.[20] Moreover, the interaction of WSe_2 with GaAs can increase the dielectric disorder, which can result in an increase in recombination centers, such as defects and localized states.[13,39]

In order to gain further insight into the properties of our 2D/3D semiconductor junction, we study the dependence of the dynamics with the excitation wavelength. Figure 2 shows the intensity of the TRDR signal as a function of the laser wavelength at 2, 10, and 50 ps in the two regions of our system, direct contact and hBN separated. We observe that optical resonance is different for the two regions: 705 nm for WSe_2/GaAs and 708 nm for the WSe_2/hBN/GaAs region. This small variation in the resonance wavelength can be due to different effects such as a local variation of the doping of the two considered regions, as well as the stress and dielectric environment differences. We also observed that the transient reflectivity of the WSe_2 in contact with GaAs is smaller, almost half, at the wavelengths of resonance of the free exciton in WSe_2 when compared to the intensity of the hBN isolated region, indicating a higher absorption of TMD in direct

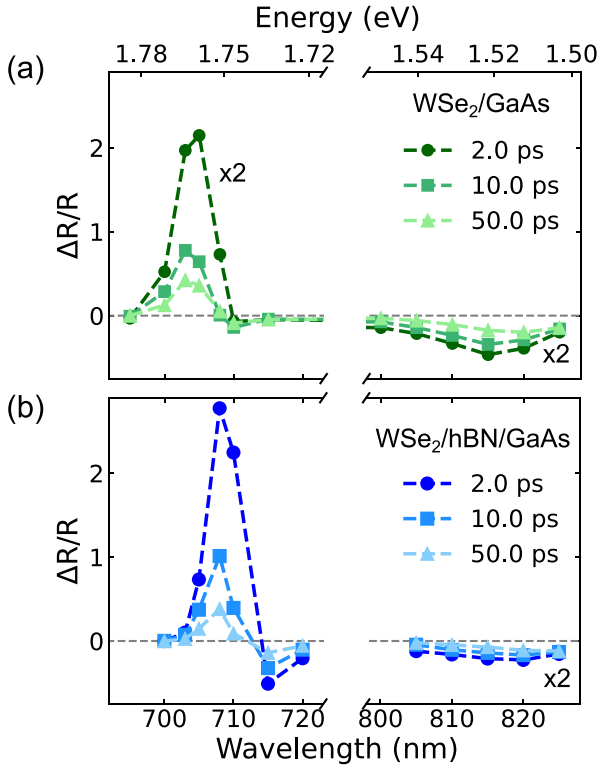

FIG. 2. (a) TRDR intensity as a function of the excitation and probing wavelengths at 2, 10, and 50 ps pump–probe delay time in WSe_2/GaAs and (b) WSe_2/hBN/GaAs. For easier comparison, the intensity values are presented as twice their real value in (a) and in the large wavelength region in (b).

contact. This response can be related to the change in the Fermi level due to the formation of the heterojunction, which reduces the electron density in TMD. Moreover, the charge transfer at the junction allows for the presence of free states in the WSe_2 conduction band, which can be accessed by the photo-excited electrons, thereby enhancing the absorption of the region. In contrast, in the hBN-isolated area, stimulated emission and photobleaching will play an important role in reducing the absorption of the flake and increasing the reflectivity. For the wavelengths in resonance with the free excitons in GaAs (800–830 nm), we observe a higher, negative, differential reflectivity in the sample in direct contact when compared to the isolated one. This observation is consistent with an increment in the photoinduced absorption of GaAs, produced by the larger density of electrons in the substrate resulting from a shift of the bands in the heterojunction.

By fitting the TRDR of the measurements for different wavelengths, we extract the energy dependence of the decay lifetimes of the two regions of interest, which are presented in Fig. 3. We did not observe any clear trend with the wavelength for the fast decay (τ_1) other than a slightly faster decay in the sample in direct contact as described previously. On the other hand, the results for the second decay time (τ_2) present a clearer trend, revealing one maximum lifetime at 705 nm for TMD in direct contact with the GaAs substrate and at 708 nm in the isolated region, which matches with the resonances of WSe_2 exciton recombination of each area. Furthermore, we observe another maximum, and the highest τ_2 value, when exciting with a wavelength of 715 nm, which is related to the signal coming from the negative, less intense, differential reflectivity in Fig. 2(b). Data points for 720 nm in the direct contact region were discarded as the signal-to-noise ratio was too low to allow fitting. Although negative signals are commonly associated with photoinduced absorption, it has also been observed that in TMDs, bandgap renormalization plays an important role in this effect.[40] Therefore, we associate the different carrier lifetimes obtained at this wavelength with the different origins of the relaxation path involved. Finally, the obtained long lifetimes (τ_3) make clear the longer-lived character of the photo-excited carriers in the TMD in direct contact with GaAs, close to the resonance.

To determine the role of thermal effects, we measured the TRDR at room temperature (Fig. 4), in the two regions of interest, exciting at the WSe_2 exciton resonance, $\lambda = 740$ nm. Our results show an overall shorter lifetime of the generated excitations when compared with the measurements at low temperature. We observe a similar behavior for both regions of the sample with just two clear decay processes: a fast decay of 9 ps and a slower decay of around 40 ps. If compared with our previous analysis at low temperature, we obtain a longer decay time τ_1, a shorter decay time τ_2, and the total absence of the presence of τ_3 decay process at room temperature. These findings are in agreement with earlier studies reporting longer decay times τ_1 of monolayer WSe_2 when increasing temperature.[26,41] One possible explanation for this phenomenon is the important role of dark states in tungsten-based TMD monolayers, which are observed, for instance, in the enhancement of the photoluminescence when increasing the temperature.[42] In our experiments at low temperature, the pump laser pulse generates hot electrons that interact with the phonons in the lattice allowing a charge transfer between WSe_2 and GaAs. When the photo-excited electrons in GaAs and holes in WSe_2 thermalize, the diminished amount of phonons reduces the carrier transition, which increases the relaxation times of both regions. At high temperatures, on the other hand, the thermally available phonons in the system facilitate new carrier relaxation pathways, which reduce the long-lived component (τ_3) of the dynamics. Another possible relaxation channel is a change in the band alignment with the temperature. In this case, the small difference in the valence band maximum considered in Fig. 1(c) could be enough for them to switch positions with the change in the temperature. Under this hypothesis, it is possible that WSe_2/GaAs could have a type-I band offset at room temperature and switch to a type-II band alignment when reducing the temperature. Further

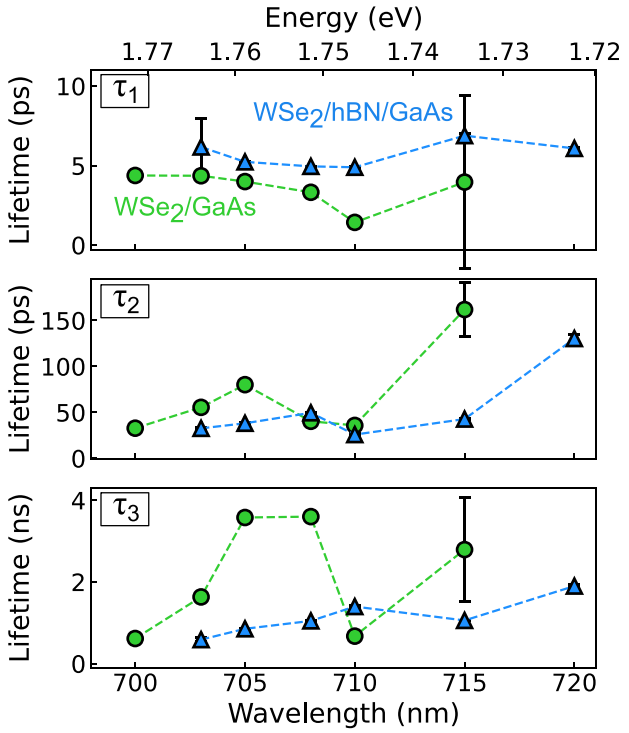

FIG. 3. Lifetimes of the TRDR signals as a function of the wavelength extracted from the three exponential decay processes described in the main text. When not shown, the error bars, obtained by the fit, are smaller than the point size.

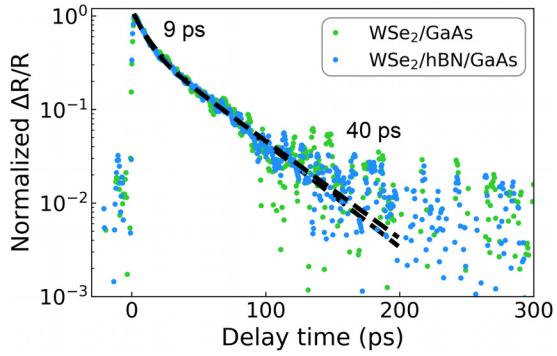

FIG. 4. Normalized TRDR for the WSe_2/GaAs (green) and WSe_2/hBN/GaAs (blue) regions at room temperature. The laser was tuned to be resonant with the WSe_2 exciton, at $\lambda = 740$ nm.

theoretical and experimental work has to be done for one to be able to pinpoint more precisely how the band alignment of this junction changes with temperature.

Our observation of a type-II band alignment and charge transfer between the prototypical 2D/3D semiconductors, WSe_2 and GaAs, at low temperatures indicates the promise of using such junctions in future optical and optoelectronic devices.[15,16,18,19] The long-lived (3.5 ns) opto-excited carriers observed here should allow for a long enough time for these carriers to be transported away from the junction region. This characteristic is one of the goals for the design of semiconductor heterojunctions, which has proven to be a determinant factor in the related optoelectronic devices.[43–45] Additionally, a long decay time is a crucial element for lasers. Therefore, the combination of a long carrier lifetime with the unique spintronic properties of both WSe_2 and GaAs such as long spin lifetimes and electric control over the spin information,[46–49] makes these junctions particularly appealing for lasers, which make use of the spin degree-of-freedom, i.e., spin lasers,[50] which have been shown to be able to operate at much higher modulation frequencies than conventional lasers.[51] We envision that such junctions, as the one shown here, using van der Waals 2D semiconductors in combination with well-established and industrially proved 3D systems, can lead to an easier uptake of 2D materials in industrial settings, leading to new device architectures.

See the supplementary material for additional experimental details regarding the fabrication, characterization, and extended TRDR measurements.

We thank J. G. Holstein, H. de Vries, F. van der Velde, H. Adema, and A. Joshua for their technical support. This work was supported by the Dutch Research Council (NWO—STU.019.014), the Zernike Institute for Advanced Materials, and the Brazilian funding agencies CNPq, FAPEMIG and the Coordenação de Aperfeiçoamento de Pessoal de Nível Superior-Brasil (CAPES)—Project code 88887.476316/2020-00. Sample fabrication was performed using NanoLabNL facilities. MHDG acknowledges the financial support of the European Union through grant ERC, 2DOPTOSPIN, 101076932. Views and opinions expressed are, however, those of the author(s) only and do not necessarily reflect those of the European Union or the European Research Council. Neither the European Union nor the granting authority can be held responsible for them.

AUTHOR DECLARATIONS

Conflict of Interest

The authors have no conflicts to disclose.

Author Contributions

Rafael R. Rojas Lopez: Conceptualization (lead); Data curation (equal); Formal analysis (lead); Investigation (lead); Methodology (lead); Project administration (equal); Software (supporting); Validation (lead); Writing – original draft (lead); Writing – review & editing (equal). **Freddie Hendriks:** Investigation (supporting); Software (lead); Validation (supporting); Writing – review & editing (supporting). **Caspar H. van der Wal:** Formal analysis (supporting); Investigation (supporting); Resources (supporting); Supervision (supporting); Writing – review & editing (supporting). **Paulo S. S. Guimaraes:** Formal analysis (supporting); Funding acquisition (supporting); Investigation (equal); Resources (supporting); Supervision (supporting); Writing – review & editing (supporting). **Marcos H. D. Guimarães:** Conceptualization (supporting); Data curation (equal); Formal analysis (supporting); Funding acquisition (lead); Investigation (supporting); Methodology (supporting); Project administration (equal); Resources (supporting); Supervision (lead); Visualization (supporting); Writing – review & editing (equal).

DATA AVAILABILITY

The data that support the findings of this study are available from the corresponding authors upon reasonable request.

REFERENCES

[1]K. F. Mak, C. Lee, J. Hone, J. Shan, and T. F. Heinz, Phys. Rev. Lett. **105**, 136805 (2010).
[2]A. Splendiani, L. Sun, Y. Zhang, T. Li, J. Kim, C.-Y. Chim, G. Galli, and F. Wang, Nano Lett. **10**, 1271 (2010).
[3]K. F. Mak and J. Shan, Nat. Photonics **10**, 216 (2016).
[4]T. C. Berkelbach, M. S. Hybertsen, and D. R. Reichman, Phys. Rev. B **88**, 045318 (2013).
[5]Y. You, X. X. Zhang, T. C. Berkelbach, M. S. Hybertsen, D. R. Reichman, and T. F. Heinz, Nat. Phys. **11**, 477 (2015).
[6]N. P. Wilson, W. Yao, J. Shan, and X. Xu, Nature **599**, 383 (2021).
[7]A. Ciarrocchi, F. Tagarelli, A. Avsar, and A. Kis, Nat. Rev. Mater. **7**, 449 (2022).
[8]S. Refaely-Abramson, D. Y. Qiu, S. G. Louie, and J. B. Neaton, Phys. Rev. Lett. **121**, 167402 (2018).
[9]A. J. Watson, W. Lu, M. H. D. Guimarães, and M. Stöhr, 2D Mater. **8**, 032001 (2021).
[10]J. Jasiński, A. Balgarkashi, V. Piazza, D. Dede, A. Surrente, M. Baranowski, D. K. Maude, M. Banerjee, R. Frisenda, A. Castellanos-Gomez, A. F. i Morral, and P. Plochocka, 2D Mater. **9**, 045006 (2022).
[11]M. Buscema, G. A. Steele, H. S. J. van der Zant, and A. Castellanos-Gomez, Nano Res. **7**, 561 (2014).
[12]Y. Sun, R. Wang, and K. Liu, Appl. Phys. Rev. **4**, 011301 (2017).
[13]A. Raja, L. Waldecker, J. Zipfel, Y. Cho, S. Brem, J. D. Ziegler, M. Kulig, T. Taniguchi, K. Watanabe, E. Malic, T. F. Heinz, T. C. Berkelbach, and A. Chernikov, Nat. Nanotechnol. **14**, 832 (2019).
[14]W. Zheng, X. Liu, J. Xie, G. Lu, and J. Zhang, Coord. Chem. Rev. **447**, 214151 (2021).
[15]Z. Xu, S. Lin, X. Li, S. Zhang, Z. Wu, W. Xu, Y. Lu, and S. Xu, Nano Energy **23**, 89 (2016).
[16]S. Lin, X. Li, P. Wang, Z. Xu, S. Zhang, H. Zhong, Z. Wu, W. Xu, and H. Chen, Sci. Rep. **5**, 15103 (2015).
[17]A. S. Bracker, E. A. Stinaff, D. Gammon, M. E. Ware, J. G. Tischler, D. Park, D. Gershoni, A. V. Filinov, M. Bonitz, F. Peeters, and C. Riva, Phys. Rev. B **72**, 035332 (2005).
[18]S. S. Sarkar, S. Mukherjee, R. K. Khatri, and S. K. Ray, Nanotechnology **31**, 135203 (2020).
[19]C. Jia, D. Wu, E. Wu, J. Guo, Z. Zhao, Z. Shi, T. Xu, X. Huang, Y. Tian, and X. Li, J. Mater. Chem. C **7**, 3817 (2019).
[20]R. R. Rojas-Lopez, J. C. Brant, M. S. O. Ramos, T. H. L. G. Castro, M. H. D. Guimarães, B. R. A. Neves, and P. S. S. Guimarães, Appl. Phys. Lett. **119**, 233101 (2021).
[21]K. Li, W. Wang, J. Leng, B. Sun, D. Li, H. Yang, T. Jiang, and Y. He, Appl. Surf. Sci. **500**, 144005 (2020).
[22]V. K. Sangwan and M. C. Hersam, Annu. Rev. Phys. Chem. **69**, 299 (2018).
[23]A. Castellanos-Gomez, M. Buscema, R. Molenaar, V. Singh, L. Janssen, H. S. J. van der Zant, and G. A. Steele, 2D Mater. **1**, 011002 (2014).
[24]M. H. D. Guimarães and B. Koopmans, Phys. Rev. Lett. **120**, 266801 (2018).
[25]R. R. Rojas-Lopez, F. Hendriks, C. H. van der Wal, P. S. Guimarães, and M. H. Guimarães, 2D Mater. **10**, 035013 (2023).

[26]T. Yan, X. Qiao, X. Liu, P. Tan, and X. Zhang, Appl. Phys. Lett. **105**, 101901 (2014).
[27]G. Wang, L. Bouet, D. Lagarde, M. Vidal, A. Balocchi, T. Amand, X. Marie, and B. Urbaszek, Phys. Rev. B **90**, 075413 (2014).
[28]Q. Cui, F. Ceballos, N. Kumar, and H. Zhao, ACS Nano **8**, 2970 (2014).
[29]T. Yan, S. Yang, D. Li, and X. Cui, Phys. Rev. B **95**, 241406 (2017).
[30]F. Ceballos, P. Zereshki, and H. Zhao, Phys. Rev. Mater. **1**, 044001 (2017).
[31]L. Wu, Y. Chen, H. Zhou, and H. Zhu, ACS Nano **13**, 2341 (2019).
[32]Y. Li, H. Zhou, Y. Chen, Y. Zhao, and H. Zhu, J. Chem. Phys. **153**, 044705 (2020).
[33]P. Wang, Y. Wang, A. Bian, S. Hao, Q. Miao, X. Zhang, J. He, D. He, and H. Zhao, 2D Mater. **9**, 035019 (2022).
[34]P. Zereshki, P. Yao, D. He, Y. Wang, and H. Zhao, Phys. Rev. B **99**, 195438 (2019).
[35]M. Tangi, P. Mishra, C.-C. Tseng, T. K. Ng, M. N. Hedhili, D. H. Anjum, M. S. Alias, N. Wei, L.-J. Li, and B. S. Ooi, ACS Appl. Mater. Interfaces **9**, 9110 (2017).
[36]J. Huang, T. B. Hoang, and M. H. Mikkelsen, Sci. Rep. **6**, 22414 (2016).
[37]T. Kümmell, U. Hutten, F. Heyer, K. Derr, R.-M. Neubieser, W. Quitsch, and G. Bacher, Phys. Rev. B **95**, 081304 (2017).
[38]C. Robert, D. Lagarde, F. Cadiz, G. Wang, B. Lassagne, T. Amand, A. Balocchi, P. Renucci, S. Tongay, B. Urbaszek, and X. Marie, Phys. Rev. B **93**, 205423 (2016).
[39]J. Li, M. Goryca, K. Yumigeta, H. Li, S. Tongay, and S. A. Crooker, Phys. Rev. Mater. **5**, 044001 (2021).
[40]E. A. A. Pogna, M. Marsili, D. De Fazio, S. Dal Conte, C. Manzoni, D. Sangalli, D. Yoon, A. Lombardo, A. C. Ferrari, A. Marini, G. Cerullo, and D. Prezzi, ACS Nano **10**, 1182 (2016).
[41]M. A. Akmaev, M. V. Kochiev, A. I. Duleba, M. V. Pugachev, A. Y. Kuntsevich, and V. V. Belykh, JETP Lett. **112**, 607 (2020).
[42]X.-X. Zhang, Y. You, S. Y. F. Zhao, and T. F. Heinz, Phys. Rev. Lett. **115**, 257403 (2015).
[43]Z. Zheng, X. Zu, Y. Zhang, and W. Zhou, Mater. Today Phys. **15**, 100262 (2020).
[44]P. Rivera, J. R. Schaibley, A. M. Jones, J. S. Ross, S. Wu, G. Aivazian, P. Klement, K. Seyler, G. Clark, N. J. Ghimire *et al.*, Nat. Commun. **6**, 6242 (2015).
[45]A. Balapure, J. R. Dutta, and R. Ganesan, RSC Appl. Interfaces **1**, 43–69 (2023).
[46]I. Žutić, J. Fabian, and S. Das Sarma, Rev. Mod. Phys. **76**, 323 (2004).
[47]X. Xu, W. Yao, D. Xiao, and T. F. Heinz, Nat. Phys. **10**, 343 (2014).
[48]G. Salis, Y. Kato, K. Ensslin, D. Driscoll, A. Gossard, and D. Awschalom, Nature **414**, 619 (2001).
[49]Z. Gong, G.-B. Liu, H. Yu, D. Xiao, X. Cui, X. Xu, and W. Yao, Nat. Commun. **4**, 2053 (2013).
[50]I. Žutić, G. Xu, M. Lindemann, P. E. F. Junior, J. Lee, V. Labinac, K. Stojšić, G. M. Sipahi, M. R. Hofmann, and N. C. Gerhardt, Solid State Commun. **316–317**, 113949 (2020).
[51]M. Lindemann, G. Xu, T. Pusch, R. Michalzik, M. R. Hofmann, I. Žutić, and N. C. Gerhardt, Nature **568**, 212 (2019).